



Lipid nanoparticles of Type-A CpG D35 suppress tumor growth by changing tumor immune-microenvironment and activate CD8 T cells in mice

Lisa Munakata^{a,1}, Yoshihiko Tanimoto^{b,1}, Akio Osa^{c,1}, Jie Meng^b, Yasunari Haseda^b, Yujiro Naito^c, Hiroto Machiyama^c, Atsushi Kumanogoh^c, Daiki Omata^a, Kazuo Maruyama^d, Yasuo Yoshioka^{e,f,g}, Yoshiaki Okada^f, Shohei Koyama^c, Ryo Suzuki^{a,*,2}, Taiki Aoshi^{b,g}

^a Laboratory of Drug and Gene Delivery Research, Faculty of Pharma-Science, Teikyo University, Japan

^b Vaccine Dynamics Project, BIKEN Innovative Vaccine Research Alliance Laboratories, Research Institute for Microbial Diseases, Osaka University, Japan

^c Department of Respiratory Medicine and Clinical Immunology, Graduate School of Medicine, Osaka University, Japan

^d Laboratory of Ultrasound Theranostics, Faculty of Pharma-Science, Teikyo University, Japan

^e Vaccine Creation Project, BIKEN Innovative Vaccine Research Alliance Laboratories, Research Institute for Microbial Diseases, Osaka University, Japan

^f Graduate School of Pharmaceutical Sciences, Osaka University, Japan

^g BIKEN Center for Innovative Vaccine Research and Development, The Research Foundation for Microbial Diseases of Osaka University, Suita, Osaka, Japan

ARTICLE INFO

Keywords:

CpG
Lipid nanoparticle
Cancer immunotherapy
Oligodeoxynucleotide delivery
Microfluidics

ABSTRACT

Type-A CpG oligodeoxynucleotides (ODNs), which have a natural phosphodiester backbone, is one of the highest IFN- α inducer from plasmacytoid dendritic cells (pDC) via Toll-like receptor 9 (TLR9)-dependent signaling. However, the in vivo application of Type-A CpG has been limited because the rapid degradation in vivo results in relatively weak biological effect compared to other Type-B, -C, and -P CpG ODNs, which have nuclease-resistant phosphorothioate backbones. To overcome this limitation, we developed lipid nanoparticles formulation containing a Type-A CpG ODN, D35 (D35LNP). When tested in a mouse tumor model, intratumoral and intravenous D35LNP administration significantly suppressed tumor growth in a CD8 T cell-dependent manner, whereas original D35 showed no efficacy. Tumor suppression was associated with Th1-related gene induction and activation of CD8 T cells in the tumor. The combination of D35LNP and an anti-PD-1 antibody increased the therapeutic efficacy. Importantly, the therapeutic schedule and dose of intravenous D35LNP did not induce apparent liver toxicity. These results suggested that D35LNP is a safe and effective immunostimulatory drug formulation for cancer immunotherapy.

1. Introduction

Conventional cancer immunotherapies focusing on increasing tumor-specific T cell responses using antigen/peptide- or dendritic cell-based vaccine have shown only limited clinical efficacies, potentially due to tumor-mediated immune suppression [1]. Recent introduction of immune checkpoint inhibitors, which release the tumor-mediated T cell suppression, has been shown substantial therapeutic effect. In some patients, this has significantly improved the overall survival [2,3]. One

of the fundamental limitation of the immune checkpoint inhibitors is the requirement for pre-existing antitumor T cell responses, which many patients do not have [1,2].

To augment antitumor immunity, several immunomodulators including cytokines such as IFN- α and IL-12 [4,5], and toll-like receptor agonists such as TLR4, TLR3, TLR7, and TLR9 [6–8] have been examined in clinical trials, and some were successfully approved for clinical use. However, these immunomodulators also have limitations for cancer therapy due to the associated intolerable toxicities [9–11].

Abbreviations: DiR, 1,1'-dioctadecyl-3,3',3'-tetramethylindotricarbocyanine iodide; DPPC, 1,2-dipalmitoyl-sn-glycero-3-phosphocholine; DOTAP, 1,2-dioleoyl-3-trimethylammonium-propane; DOPE, 1,2-dioleoyl-sn-glycero-3-phosphoethanolamine; D35LNP, D35-containing lipid nanoparticles; LPS, lipopolysaccharides; DSPE-PEG(2k or 5k), N-(Carbonyl-methoxypolyethyleneglycol (2000 or 5000)-1,2-distearoyl-sn-glycero-3-phosphoethanolamine); TLR9, toll-like receptor 9; BM, bone marrow; hPBMcs, human peripheral blood mononuclear cells; iMonocytes, inflammatory monocytes; ODNs, oligodeoxynucleotides; PFA, paraformaldehyde; pDC, plasmacytoid dendritic cells; PMNs, polymorphonuclear cells; TANS, tumor-associated neutrophils

* Corresponding author at: 3-1 Yamadaoka, Suita, Osaka, 565-0871, Japan.

E-mail addresses: r-suzuki@pharm.teikyo-u.ac.jp (R. Suzuki), aoshi@biken.osaka-u.ac.jp (T. Aoshi).

¹ The authors contributed equally to this work.

² Co-corresponding authors.

<https://doi.org/10.1016/j.jconrel.2019.09.011>

Received 6 June 2019; Received in revised form 10 September 2019; Accepted 18 September 2019

Available online 16 October 2019

0168-3659/© 2019 The Authors. Published by Elsevier B.V. This is an open access article under the CC BY-NC-ND license (<http://creativecommons.org/licenses/by-nc-nd/4.0/>).

CpG motif-containing oligodeoxynucleotides (ODNs) have been investigated as immunomodulatory and immunostimulatory drugs, which are TLR9 agonists and induce innate immune responses such as interferon and inflammatory cytokine secretions. Four types of CpG ODNs have been reported including Type-A, B, C, and P [12,13]. Type-A CpG ODNs mostly consist of a natural phosphodiester backbone, and they strongly induce IFN- α production from plasmacytoid dendritic cells (pDCs). Type-B CpG ODNs consist of an unnatural phosphorothioate backbone, and they mainly activate B cells and induce IL-6 production. Type-C CpG ODNs also consist of an unnatural phosphorothioate backbone, and they mainly induce IL-6 production from B cells, but an introduction of one palindromic sequence enables weak IFN- α induction. Type-P CpG ODNs similarly consist of an unnatural phosphorothioate backbone as Type-B and C, but they contain 2 palindromic sequences, which contribute to induce strong IFN- α as well as IL-6 production. The most popular CpG ODNs examined in the clinical studies are Type-B CpG ODNs; however, repeated Type-B CpG ODNs administration caused splenomegaly, lymphoid follicle destruction, and liver toxicity in mice [14–16], and hematologic adverse events, injection site reaction, and influenza-like symptoms in human cancer clinical trials with no additional benefit [17,18]. This Type-B associated toxicity has been shown to be associated with TLR9 signaling (dependent on the presence of CpG motif), but some are derived from the unnatural phosphorothioate backbones. ODNs consisting of a phosphorothioate backbone including Type-B, C, and P CpG ODNs are known to bind various proteins in nonspecific ways [19,20], causing various effects such as platelet activation [21], complement activation [22], and clotting time prolongation [23,24], raising safety concerns. In contrast, Type-A CpG ODNs is composed of mostly the natural phosphodiester backbone, freeing from the above-mentioned phosphorothioate-associated side effects, and would be an attractive therapeutic candidate for cancer immunotherapy.

However, the use of Type-A CpG ODNs for cancer treatment has been very limited [25,26]. One of the reasons for the unavailability of Type-A CpG ODNs-based drugs for cancer therapy is the requirement of a natural phosphodiester backbone for high IFN- α -inducing activity [27], which is also associated with rapid *in vivo* degradation due to its susceptibility to DNase. In addition, the handling of D35 is very difficult because of the formation of uncontrolled large aggregates in salt-containing buffers such as saline and PBS [20,28,29]. Moreover, the negatively charged phosphodiester backbone of D35 does not bind to cell membranes due to the electrostatic repulsion between nucleic acids and the cell membrane, which results in poor cellular uptake [30]. To overcome these limitations of D35 for immunotherapeutic drug application, development of practical drug delivery system for D35 is demanded.

In this study, we developed a lipid-based drug delivery system for Type-A CpG ODN D35, and found that lipid nanoparticle formulation [31] is a promising pharmaceuticalization method. Evaluation of the anti-tumor effect and potential toxicity in mice demonstrated that our developed D35-containing lipid nanoparticles (D35LNP) formulation is a safe and promising immunostimulatory drug, especially for cancer immunotherapy. D35LNP also showed a combinational effect with an immune checkpoint inhibitor.

2. Materials and methods

2.1. Materials

D35 [28] was purchased from GeneDesign (Osaka, Japan). 1,2-dioleoyl-3-trimethylammonium-propane (DOTAP) was purchased from Lipoid GmbH. 1,2-Dipalmitoyl-sn-glycero-3-phosphocholine (DPPC), 1,2-dioleoyl-sn-glycero-3-phosphoethanolamine (DOPE), and N-(Carbonyl-methoxypolyethyleneglycol (2000 or 5000)-1,2-distearoyl-sn-glycero-3-phosphoethanolamine (DSPE-PEG(2k or 5k)) were purchased from NOF CORPORATION, Tokyo, Japan. Cholesterol was purchased

from FUJIFILM Wako Pure Chemical Corporation, Ltd., Osaka, Japan.

2.2. Preparation of D35-lipid nanoparticles (LNP)

D35LNP was prepared with NanoAssemblr Benchtop (Precision NanoSystems Inc., BC, Canada) which can mediate bottom-up self-assembly for nanoparticle synthesis with microfluidic mixing technology. Briefly, lipids were dissolved in ethanol. Lipid components were changed in each experiment such as DOTAP: DPPC: Cholesterol: DSPE-PEG(2k) = 50: 19.5:14: 30: 0.5–6, DOTAP: DPPC: Cholesterol: DSPE-PEG(5k) = 50: 19.5: 30: 0.5 or DOTAP: DOPE: Cholesterol: DSPE-PEG(2k) = 50: 19.5: 30: 0.5. D35 was prepared in 25 mM acetate buffer at pH 4.0. The lipid solution (10 mg/mL) in ethanol and D35 solution were injected into the microfluidic mixer at a 1:3 vol respectively combined final flow rate of 15 mL/min (3.75 mL/min ethanol, 11.25 mL/min aqueous). The D35LNP mixtures were immediately dialyzed (50 kD MWCO dialysis tubing, Repligen Corporation, MA) against 5% glucose solution to remove ethanol and unload D35. D35LNP was then concentrated to approximately 0.7 mg/mL D35 using Amicon Ultra centrifugal filters (100 kD MWCO, Merck KGaA, Darmstadt, Germany) and filtered through a 0.22 μ m PVDF filter (Merck KGaA). The theoretical D35-to-lipid ratios for all formulations were maintained at N/P charge ratios (ratios of the charge on the cationic lipid, assuming it is in the positively charged protonated form, to the negative charge on the D35 oligonucleotide) of 3. All LNP preparation work was carried out at room temperature.

2.3. Analysis of lipid nanoparticles

The size distribution of D35LNP was measured with dynamic light scattering (Zetasizer Nano-ZS, Malvern Panalytical Ltd., UK). The morphology of D35LNP was measured through negative staining (2% phosphotungstic acid) using transmission electron microscope (TEM (JEM-1200EX at 80 kV), JEOL Ltd., Tokyo, Japan). The TEM images were taken at the Hanaichi UltraStructure Research Institute (Aichi, Japan). D35 concentration in D35LNP suspension was measured with picogreen reagent. Briefly, D35LNP was incubated at 37 °C for 10 min in the presence of 1% Triton X-100 (Wako Pure Chemical Industries), and picogreen reagent was added. The fluorescence intensity (Ex/Em: 485/528 nm) was measured.

2.4. Human PBMCs

PBMCs were prepared from Japanese healthy adult volunteers with informed consent. All experiments using human PBMCs were approved by the Institutional Review Board of the Research Institute for Microbial Diseases, Osaka University (Permit number: 26-5). After preparing PBMCs using Ficoll-Paque PLUS (GE) and LeucoSep (Greiner), it was washed twice with RPMI 1640 medium, and resuspended in R-10 medium (RPMI 1640 medium supplemented with 10% fetal calf serum, 100 unit/mL penicillin, and 100 μ g/mL streptomycin). PMN cells were isolated from human whole blood using Polymorphprep™ according to the manufacturer's instruction. For B cells, pDCs, and monocytes isolation, each cell population was positively selected using CD19, CD304, and CD14 magnetic MicroBeads (Miltenyi) according to the manufacturer's instruction.

2.5. Mice

C57BL/6 mice were purchased from Sankyo Labo Service Corporation Inc. or CLEA Japan. TLR7 and TLR9 KO mice were purchased from Oriental Bio Service Inc. Mice (6–10-week-old) were used in all experiments. All animal experiments were approved according to the Teikyo University guidelines for the welfare of animals in studies of experimental neoplasia, the Animal Care and Use Committee of Osaka University. The experiment was carried out according to the

Regulations on Animal Experiments at Teikyo University and Osaka University.

2.6. Mouse BM cells

The femurs and the tibiae of mice were removed and the bones were cleaned from the surrounding muscle tissues by scissors. The marrow was flushed out with RPMI 1640 using a syringe with a 25 G needle. The cells were treated with ACK lysis buffer for 5 min. After washing the cells once in RPMI 1640 and counting the cell number, bone marrow (BM) cells were resuspended in R-10 medium. To enrich or deplete mouse pDCs in BM cells, Plasmacytoid Dendritic Cell Isolation Kit (Miltenyi) was used. The flow-through cells were used as pDC-enriched cells and the column-trapped cells were used as pDC-depleted cells.

2.7. In vitro stimulation

Human PBMC or mouse BM cells were plated on 96-well plates at 1×10^6 cells/well/200 μ L. D35 (1 μ M = 6.3 μ g/mL), D35LNP (1 μ g/mL as D35 amount), or R848 (1 μ g/mL) (InvivoGen) was added to the cell cultures overnight at 37 °C in CO₂ incubator. The centrifuged supernatant was collected and used for cytokine ELISA. Human IFN- α was measured with Human IFN- α pan ELISA development kit (Mabtech). Mouse IFN- α / β (type I IFN) production was measured using B16-Blue IFN- α / β reporter cells (InvivoGen). Mouse IL-6 production was measured with Mouse IL-6 DuoSet ELISA (R&D Systems).

2.8. MC38 cells

The MC38 cell line was cultured with high glucose DMEM (Nacalai Tesque) containing 10% fetal bovine serum (FBS, Gibco), L-glutamine, MEM Nonessential Amino Acids Solution (Nacalai Tesque), penicillin/streptomycin (Nacalai Tesque) and gentamicin (50 μ g/mL, Nacalai Tesque) in 10 cm polystyrene tissue culture dishes at 37 °C in a 5% CO₂ incubator.

2.9. Tumor treatment

Mice were intradermally inoculated with MC38 (1×10^6 cells), due to this inoculation amount was used for immunotherapeutic evaluations of several immune checkpoint inhibitors and their combinations [32,33]. D35LNP was intratumorally (4.5 μ g/mouse as D35 amount) or intravenously (25 μ g/mouse as D35 amount) injected three times a week from day7-9 to day17-20. For CD8 T cell depletion experiments, anti-CD8 α (clone 53-6.7 (rat IgG)) (100 μ g/mouse) (Bio X cell, NH) and isotype control antibody (normal rat IgG, Thermo Fisher Scientific, MA) (100 μ g/mouse) were injected intraperitoneally at days 6 and 13 after tumor inoculation. For D35LNP and immune checkpoint antibody combination experiment, anti-PD-1 antibody (clone: 29 F.1A12) (200 μ g/mouse) and isotype control antibody (clone: 2A3) (200 μ g/mouse) (both were purchased from Bio X cell, NH) were injected intraperitoneally at the same days as D35LNP administration. Tumor size was measured using calipers, and tumor volume was calculated using the following formula: (major axis \times minor axis²) \times 0.5 [34].

2.10. Immunostaining

The MC38 tumors were embedded in O.C.T. Compound (Sakura Finetek), and sections were prepared using Cryostat (Leica CM3050 s). The sections were fixed in 4% paraformaldehyde (PFA)-PBS (Nacalai Tesque) for 5 min, and washed 3 times and blocked with TBS (Thermo fisher scientific). The samples were stained with the following fluorescent dye and antibodies. The nuclei were stained with DAPI (Dojindo, 0.25 μ g/ml), the blood vessels were stained with anti-mouse CD31-Alexa Fluor 647 (BioLegend, Clone: MEC13.3, 1:100) and the CD8 T

cells were stained with anti-mouse CD8b-PE (BioLegend, Clone: YTS156.7.7, 1:100).

2.11. mRNA transcription measurement

The MC38 tumors were embedded in O.C.T. Compound (Sakura Finetek), and sections were prepared using Cryostat. Total RNA was extracted from the frozen section using NucleoSpin RNA (Takara Bio), and cDNA strands were generated with ReverTra Ace qPCR RT Kit (TOYOBO). Real-time PCR was performed with LightCycler 480 II (Roche) using KAPA SYBR FAST qPCR Master Mix Kit (NIPPON Genetics). Expression of target mRNA was normalized to expression of reference mRNA (GAPDH), and fold change was calculated based on the $\Delta\Delta$ Ct method [35]. The primers related to tumor marker were designed by Universal ProbeLibrary Assay Design Center (Roche, ProbeFinder Version: 2.53), and each primer sequence is described in Supplementary Table 1. The primers for examining gene expression of TCRV α and β repertoires were designed based on a previous study [36], and each primer sequence is described in Supplementary Table 2.

2.12. Immune cell isolation and Immune profiling using flow cytometry

The protocol of immune cell isolation has been described in previous study [37]. Briefly, MC38 tumor was resected and weighed, then shredded into small pieces and incubated in dissociation buffer including 100 U/mL of collagenase type IV (Invitrogen), and 100 μ g/mL of DNase I (Roche) for 45 min. After incubation, tumor cells were treated with red blood cell lysis buffer (Gibco), and cell suspensions were made to pass through a 100- μ m cell strainer (Falcon). The cell pellet was dissolved with 2% FBS in PBS and was used for flow cytometry analysis. Isolated cells were stained using the LIVE/DEAD Fixable Dead Cell Stain Kit (Invitrogen). After Fc blocking (clone: 2.4G2) (BD Biosciences), cells were subsequently stained with antibodies for surface antigens listed in Supplementary Table 3. Fixation/permeabilization buffers (Invitrogen by Thermo Fisher Scientific) were used for intracellular staining. Sample acquisition was performed on a BD FACS Canto II cytometer equipped with Diva software and analyzed using FlowJo. Gating strategy for identifying immune cell populations was performed as described previously [38].

2.13. IVIS

D35LNP was labeled with lipophilic carbocyanine DiOC18 (7) (DiR) (1,1'-Dioctadecyl-3,3,3',3'-tetramethylindotricarbocyanine iodide, Thermo Fischer Scientific Inc., MA). Briefly, DiR solution in ethanol was added into the D35LNP suspension (DiR/total lipid of D35LNP: 1.6 mg/60 mg), and DiR-labeled D35LNP (DiR-D35LNP) was prepared. In the prepared DiR-D35LNP, we confirmed that the remaining free DiR was only less than 1% of initial concentration, and the particle size and distribution was not changed compared with non-labeled D35LNP by ultrafiltration and dynamic light scattering, respectively. Mice were subcutaneously injected with MC38 cells (1×10^6). DiR-D35LNP was intravenously (D35: 25 μ g/mouse) injected. After 6 h, the mice were sacrificed, and the tissues were collected from the mice. The tissues were observed with fluorescence imaging system (Ex/Em: 745/830 nm) (IVIS imaging system (Lumina XR), PerkinElma Inc., MA) and the signal intensity was calculated using Living Image Software (PerkinElma Inc.).

2.14. Liver toxicity

D35 (25 μ g/mouse) or D35LNP (25 μ g/mouse as D35 amount) was intravenously injected into the mice. Lipopolysaccharides (LPS) (25 μ g/mouse) from *Escherichia coli* O111:B4 (Merck KGaA) was injected through the tail vein of C57BL/6 J mice as positive control of liver toxicity. After 1 day, the mice were sacrificed, and the blood was collected from tail vein by using heparin-treated glass capillary tubes. The

liver was fixed in 10% Formalin Neutral Buffer Solution, Deodorized (Mildform 10 N (FUJIFILM Wako Pure Chemical Industries, Ltd.)), and embedded in paraffin. The slices were prepared with paraffin sectioning method, stained with hematoxylin-eosin, and assessed in Kamakura Techno-Science Inc. (Kamakura, Japan). ALT or AST level in the blood (plasma) samples was measured with Transaminase CII-test Wako (FUJIFILM Wako Pure Chemical Industries, Inc.). We also assessed the liver toxicity after repeated D35LNP injection. In this experiment, D35 (25 µg/mouse) or D35LNP (25 µg/mouse as D35 amount) was intravenously injected into mice 5 times every 2 days. After 2 days of the final injection, the blood and the liver were collected, and the liver toxicity was assessed the same way as described above.

2.15. Statistical analysis

The data were presented as mean \pm SD, and One-way analysis of variance (ANOVA) with Tukey or Bonferroni test were used to analyze the tumor growth and liver enzyme data when more than two groups were compared. Two group comparison was analyzed by Student's *t*-test. Gene expression data were presented as mean \pm SEM and analyzed with Mann-Whitney U test. All Statistics were calculated with BellCurve for Excel (Ver. 3.00; Social Survey Research Information Co., Ltd.) or Prism software (GraphPad Ver. 7.01).

3. Results

3.1. Development of the drug delivery system for Type-A CpG D35

To develop an efficient drug delivery system for D35, we focused on a lipid-based drug delivery system. We prepared substantial numbers of neutral, cationic, and anionic lipid based complexes with D35, and carefully tested these lipid/D35 complexes. Through in vitro evaluations of size, stability, and cytokine production from human peripheral blood mononuclear cells (hPBMCs), we practically chose DOTAP, a cationic lipid as the main lipid component, and cholesterol and DPPC as the other components (see Methods) to make the particulate D35/lipid complex. As described later in this study, DOTAP based D35/lipid complex formed the lipid nanoparticles (referred to as D35LNP) (Fig. 1H and I). We also tested various amounts (mol%) and lengths of PEG-lipid incorporations. Successfully prepared samples were further evaluated for their IFN- α inducing ability from both hPBMCs (Fig. 1A) and mouse bone marrow (BM) cells (Fig. 1B). Among them, 0.5% of 2K-PEG-lipid incorporated D35LNP showed the most effective and consistent IFN- α production from both human and mouse BM cells (Fig. 1A and B). An increased amount of 2K-PEG mol% resulted in decreased IFN- α production, suggesting the “PEG dilemma” [39] phenomenon. When 5K-PEG-lipid was examined, 0.5% of 5K-PEG-lipid incorporated D35LNP was consistently less effective than 0.5% of 2K-PEG-lipid incorporated D35LNP (Fig. 1A and B). Based on these results, we chose 0.5% of 2K-PEG-lipid incorporated D35LNP (D35LNP0.5%), and occasionally 3.0% of 2K-PEG-lipid incorporated D35LNP (D35LNP3.0%) for further evaluation.

Next, we examined the molecular and cellular mechanisms of the D35LNP-mediated IFN- α induction. IFN- α induction with D35LNP was completely dependent on the presence of CpG-motif in the D35 sequence (Fig. 1C). When CpG-motif was replaced with GpC-motif (not stimulatory for TLR9), IFN- α induction ability was diminished in both human PBMCs (Fig. 1C; left panel) and mouse BM cells (Fig. 1C; right panel). In addition, incorporation of pH-sensitive-endosome-disrupting lipid DOPE [40] reduced IFN- α induction to about 50% (Fig. 1D). In accordance with these results, IFN- α induction with D35LNP was completely dependent on TLR9 but not TLR7, using TLR9 and TLR7 (as control)-deficient BM cells from mice (Fig. 1E). We also enriched or depleted pDC from wild type mouse BM cells and stimulated them with D35LNP0.5%. IFN- α induction remained higher in pDC enriched BM cells, but diminished in pDC depleted BM cells (Fig. 1F). Similar results

were obtained with human PBMCs. IFN- α induction was only detected in CD304⁺ pDC population, but not in polymorphonuclear cells (PMNs), CD19⁺ B cells, and CD14⁺ monocytes (Fig. 1G). These results demonstrated that D35LNP induced IFN- α secretion via endosomal TLR9 signaling and pDC dependent manner, as lipid free non-particulate original D35.

We next examined the physical property of these D35LNPs. D35LNP showed narrow size distribution. The average sizes of D35LNP0.5% and D35LNP3.0% were 54.0 nm (polydispersity index (PDI): 0.157) and 43.0 nm (PDI: 0.089), respectively (Fig. 1H), which were determined through dynamic light scattering measurement. Their zeta potentials were 1.12 ± 8.26 mV and 0.34 ± 11.2 mV, respectively, indicating that D35LNP had slightly positive or almost neutral surface charge under physiological condition despite containing 50% cationic lipid DOTAP. Transmission electron microscope revealed that both D35LNP0.5% and D35LNP3.0% were spherical in shape with fully filled packed core, indicating that our developed D35LNPs formed lipid nanoparticles (Fig. 1I).

3.2. D35LNP0.5% showed anti-tumor effect via intratumoral injection

We next examined D35LNPs in vivo using tumor model in mice. MC38 tumor cells (murine colon adenocarcinoma) were inoculated subcutaneously, and the mice were treated with D35LNPs through intratumoral (i.t.) injection at days 9, 11, 13, 15, and 17 after tumor inoculation (Fig. 2A; upper). The tumor growth was significantly suppressed with D35LNP0.5% treatment at the time point of days 17 and 21 compared with non-treated group, while D35LNP3.0% did not show apparent therapeutic effect at all examined time points (Fig. 2B), suggesting “PEG dilemma” [39] that also affects in vivo bioactivity of D35LNP. This difference in therapeutic effect was consistent with the difference in IFN- α inducing ability in vitro between D35LNP0.5% and D35LNP3.0% (Fig. 1B). Lipid free D35 showed no tumor suppressive effect at all (Fig. 2B).

Next, we tested whether the anti-tumor effect of D35LNP0.5% was dependent on CD8 T cells. CD8 T cell depletion with anti-CD8a antibody treatment exacerbated tumor progression without any other treatment (Fig. 2C; CD8a-Ab), while isotype control antibody administration showed minimal effect on tumor growth compared to that in the non-treated group (Fig. 2C and D; Isotype-Ab). With D35LNP0.5% i.t. treatment, tumor growth was significantly suppressed compared to that in the non-treated group at day 21, and CD8 T cell depletion with anti-CD8a antibody completely canceled D35LNP0.5%-mediated anti-tumor effect (Fig. 2C and D; D35LNP0.5% + CD8a-Ab).

Histological examination of tumor at day 21 supported that anti-CD8a antibody administration depleted CD8 T cells completely in the tumor tissue (Fig. 2E). Although MC38 tumor contains many CD8 T cell infiltrations without any treatment, CD8 T cell infiltration in the tumor was more aggressive with D35LNP0.5% i.t. treatment (Fig. 2E; D35LNP0.5%). Collectively these results suggested that D35LNP0.5% i.t. injection resulted in CD8 T cell activation at the tumor site, which effectively suppressed tumor growth.

3.3. D35LNP0.5% changes gene expression in the tumor microenvironment

To examine immune related gene expression change at the tumor site after D35LNP0.5% i.t. injection, we purified the mRNA of tumors from groups shown in the Fig. 2C at day 21. The gene expression induction of interferon, chemokine, tumor microenvironment, and T cell differentiation type such as Th1-, Th2-, Th17-, and Treg- related genes were determined by real-time PCR. Among these, *Ifna6*, *Ifnb1*, *Ifng*, *Cxcl9*, *Cxcl10*, *Cxcr3*, *Cd274* (PD-L1), *Stat4*, *Stat6*, *Il6*, *Il1b*, and *Tgfb1* significantly increased in the D35LNP0.5%-treated group (n = 5) (Fig. 3A) compared to non-treated group (n = 5). Notably, overall gene expression levels of *Ifng*- and Th1-related genes were substantially higher than those of Th2-, Th17-, and Treg-related genes (Fig. 3A). A

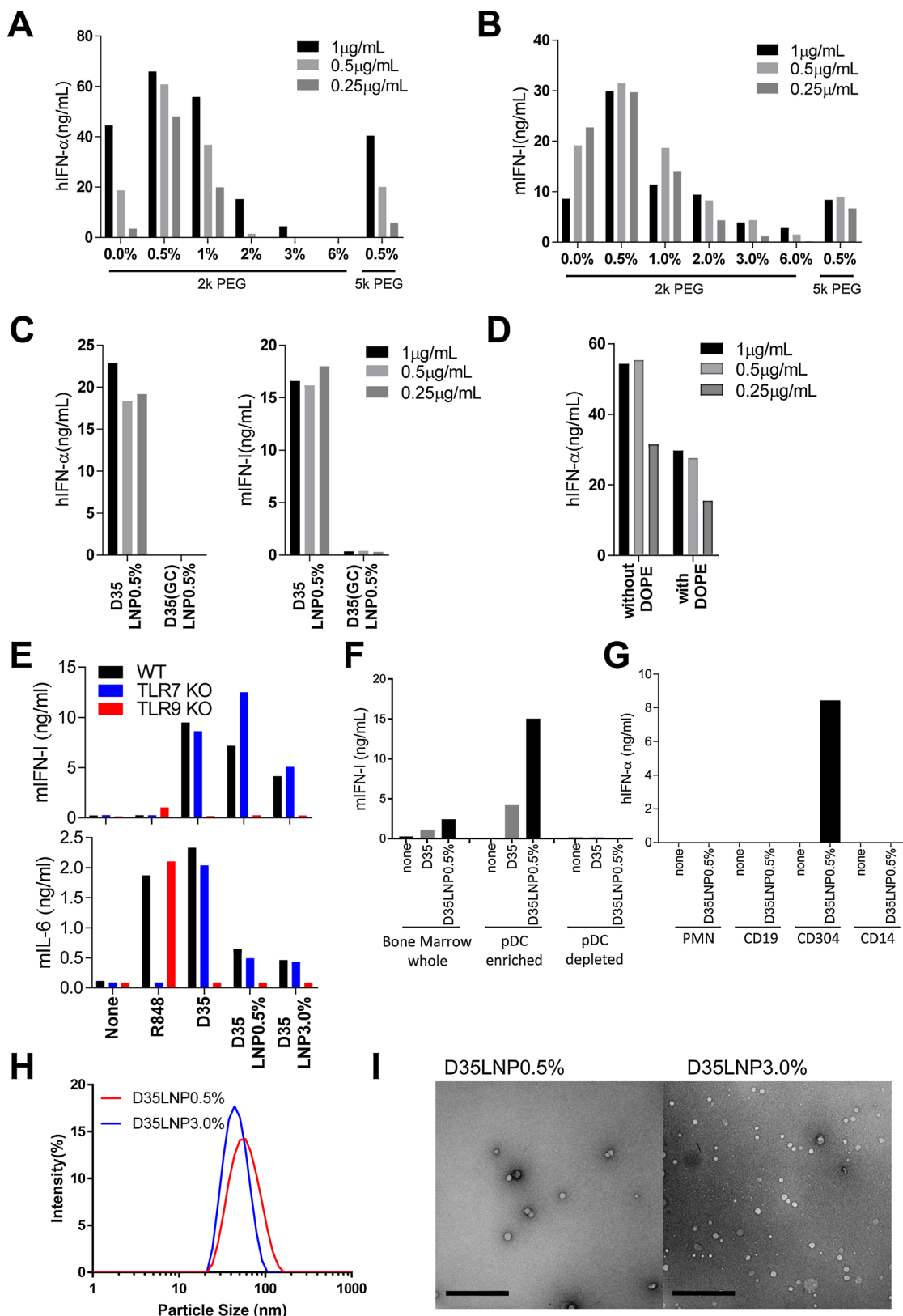


Fig. 1. Development of lipid nanoparticle for Type-A CpG D35.

(A–B) IFN-α production from human PBMCs (A) or mouse bone marrow (BM) cells (B) with various amount of 2K- or 5K-PEG-lipid incorporated D35LNP stimulation in vitro. (C) CpG-motif dependency of D35LNP mediated IFN-α production in both human PBMC (left panel) and mouse BM cells (right panel). (D) Better IFN-α induction of human PBMCs without pH sensitive endosome escapable lipid DOPE, suggesting the importance of D35 delivery to the endosome. Each bar indicates IFN-α production with D35LNP stimulation (1, 0.5, and 0.25 μg/mL as D35 amount). (E) TLR9 but not TLR7 dependent IFN-α induction from mouse BM cells. R848 (1 μg/mL), D35 (1 μM = 6.3 μg/mL), and D35LNP (1 μg/mL as D35 amount). (F) pDC is a source of IFN-α in mouse BM cells stimulated with D35LNP. D35 (1 μM), and D35LNP (1 μg/mL). (G) pDC is a source of IFN-α in human PBMCs stimulated with D35LNP(1 μg/mL). (H) The size distribution measurement by dynamic light scattering of D35LNP 2K-PEG 0.5% (D35LNP0.5%) and D35LNP 2K-PEG 3.0% (D35LNP3.0%). (I) TEM image of D35LNP0.5% and D35LNP3.0%. Black bars indicate 400 nm. Bar graph indicates a representative data of at least two independent experiments with similar results.

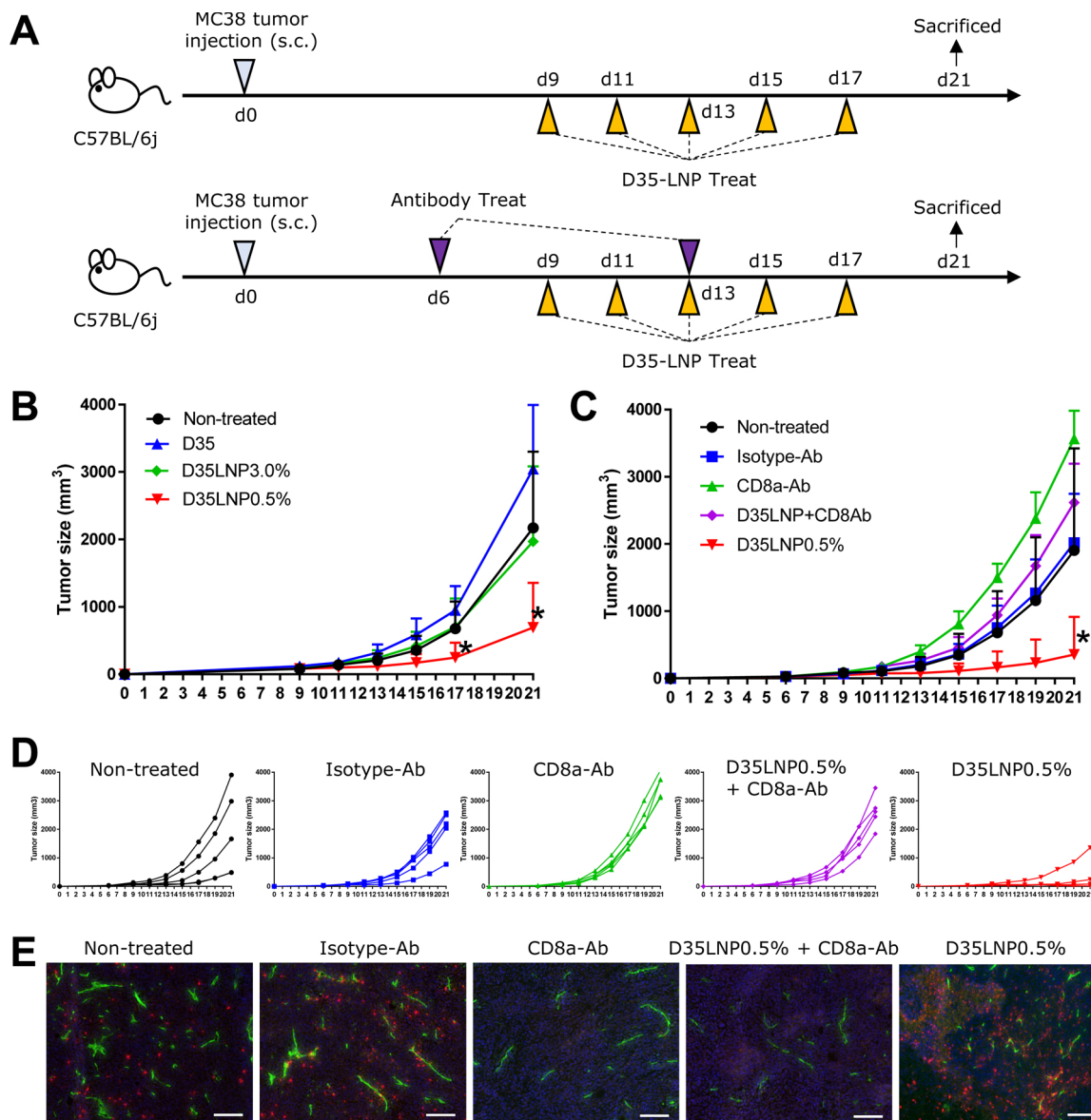


Fig. 2. Anti-tumor effect with D35LNP intratumoral treatment.

(A) Treatment procedure. C57BL/6 mice were intradermally inoculated with MC38 tumor (1×10^6 cells). D35LNP was injected intratumorally at days 9, 11, 13, 15 and 17 (A; upper panel). For CD8 T cell depletion experiment, mice were injected anti-CD8a antibody or isotype control antibody intraperitoneally (A; lower panel) in addition to D35LNP intratumoral injection at days 9, 11, 13, 15 and 17, and at days 6 and 13. (B–C) Tumor growth curves. Tumor size was measured at days 9, 11, 13, 15, 17, and 21. Values are expressed as the mean \pm S.D., and asterisk (*) means $P < 0.05$. (D) Individual tumor growth curves of Fig. 2C. (E) Immunofluorescent histology staining of MC38 tumor with nuclei (DAPI, blue), CD31 (green), and CD8b (red). Scale bars indicate 200 μ m. Note that CD8a-antibody treatment completely depleted CD8 T cells in tumor tissue. All statistical significances were calculated by one-way analysis of variance (ANOVA) with Bonferroni test.

strong increase in the expression of *Ifng*, *Cxcl9*, and *Cxcl10* suggests that D35LNP0.5% i.t. treatment provoked “T cell-inflamed” status [41,42]. *Ccl22* and *Cd274* (PD-L1) induction also suggested that the activated CD8 T cell induced regulatory mechanisms, which is affecting tumor microenvironment [43,44]. Interestingly, most of the elevated gene expressions induced by D35LNP0.5% i.t. treatment were canceled with anti-CD8a antibody treatment, whereas *Ifna6* gene expression remained high after anti-CD8a antibody treatment (Fig. 3A; *Ifna6*, D35LNP + CD8Ab vs. D35LNP). These results indicated that D35LNP0.5% i.t. injection caused initial IFN- α expression in the tumor, and then induced Th1-skewed immune-environment and CD8 T cell activation, which finally resulted in tumor growth suppression.

We also examined TCR repertoire gene expression in the tumors of both non-treated ($n = 5$) and D35LNP0.5%-treated groups ($n = 5$). The expression of TCR *Va6-5/6-7* and *Va12* genes significantly increased in

tumors treated with D35LNP0.5% i.t. compared to that in the non-treated group, while TCR repertoire gene expression in the spleen did not change in both groups (Fig. 3B). These data supported that D35LNP0.5% i.t. injection induced tumor-specific T cell responses in tumors.

3.4. D35LNP0.5% intravenous injection showed anti-tumor effect

We also tested D35LNP intravenous (i.v.) treatment against subcutaneous the MC38 tumor. Tumor growth was significantly suppressed with D35LNP0.5% i.v. treatment, while neither D35 nor D35LNP3.0% treatment was effective (Fig. 4A). Histological examinations showed no apparent differences in CD8 T cells infiltration among these groups (Fig. 4B). Although the level of gene expression was not as strong as that with i.t. treatment (Fig. 3), the expression of *Ifng*, *Cxcl9*, and *Stat4*

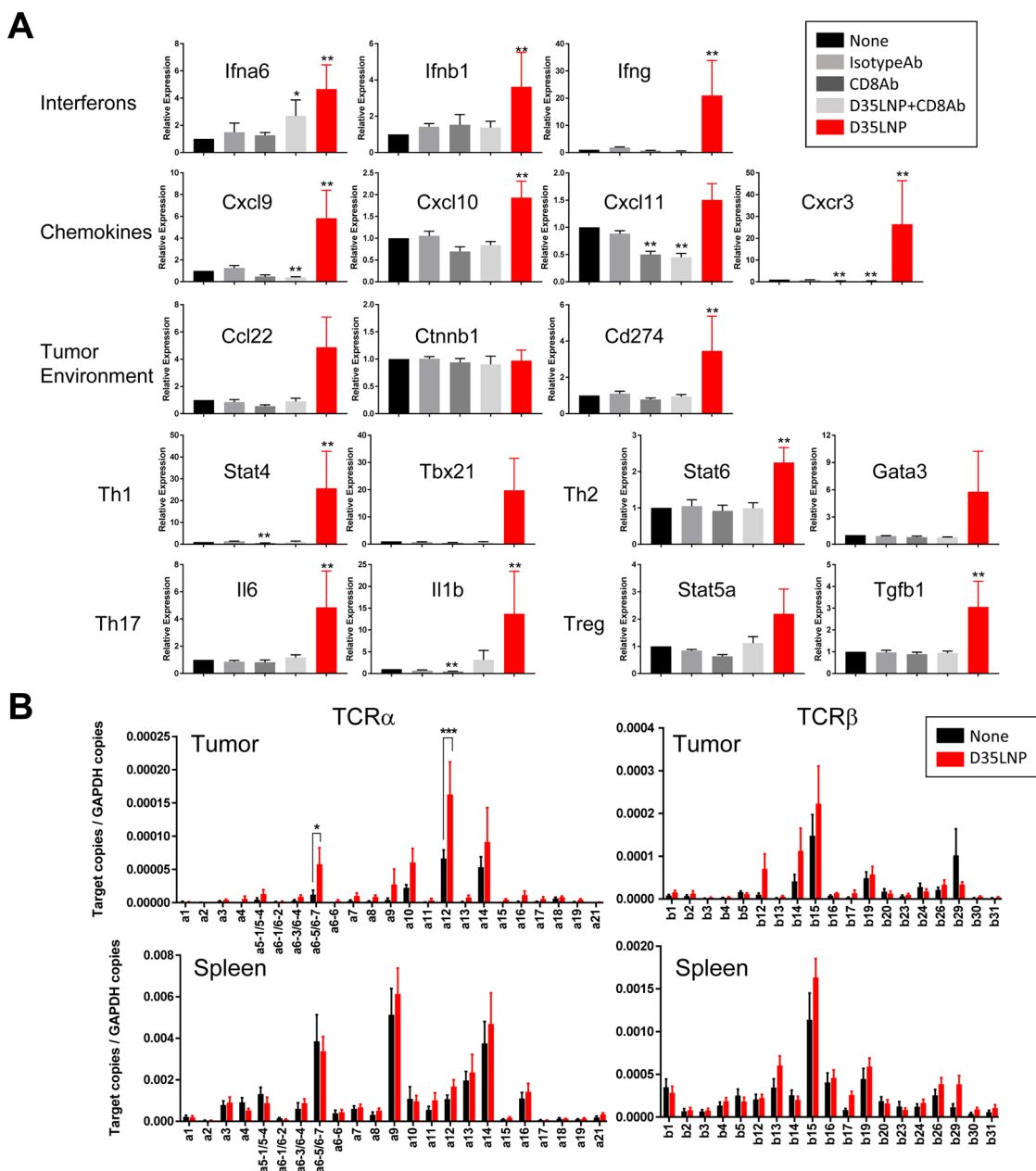


Fig. 3. Gene expression change at the tumor site with D35LNP0.5% intratumoral injection. Tumor tissues (n = 4 or 5) of each group in Fig. 2C were evaluated for mRNA expression for several panels of genes by qRT-PCR method. (A) The panels includes interferons (*Ifna6*, *Ifnb1*, *Ifng*), chemokines (*Cxcl9*, *Cxcl10*, *Cxcl11*, *Cxcr3*), tumor environment (*Ccl22*, *Ctnnb1*, *Cd274*(PD-L1))(C), Th1(*Stat4*, *Tbx21* (Tbet))(D), Th2 (*Stat6*, *Gata3*), Th17 (*Il6*, *Il1b*), and Treg (*Stat5a*, *Tgfb1*). Values are expressed as the mean ± SEM of gene expression relative to GAPDH. *P < 0.05, ***P < 0.01. (B) TCR repertoire gene expression changes in the tumor and the spleen at day 21. Black bar indicates non-treated samples, and red bar indicates D35LNP treated samples. *P < 0.05, ***P < 0.001. Statistical significance was calculated by Mann-Whitney U test.

(all of them were Th1-related genes) significantly increased in the D35LNP0.5% i.v. treated group (n = 4) compared to non-treated group (n = 5) (Fig. 4C), which is consistent with the tumor-suppressive effect (Fig. 4A). These results suggested that D35LNP0.5% i.v. treatment also induced weak but substantial Th1 skewed immune environment in tumor site, as seen in i.t. treatment (Fig. 3). We also performed D35LNP0.5% i.v. treatment with or without anti CD8a depletion antibody injection. The tumor suppressive effect by D35LNP0.5% i.v. treatment was completely canceled by CD8 T cells depletion (Fig. 4D), suggesting that D35LNP0.5% i.v. also effectively changed tumor immune-environment and activated CD8 T cells to suppress tumor growth.

3.5. Combination treatment with D35LNP0.5% and a PD-1-blocking antibody

To investigate whether D35LNP0.5% exerts a combinational effect with immune checkpoint inhibitors against MC38 tumors, MC38 subcutaneous tumor bearing mice were treated with D35LNP0.5% i.t. and/or PD-1 blocking antibody intraperitoneally (i.p.) 3 times a week between 8–20 days after tumor inoculation (Fig. 5A). The groups treated with the PD-1 antibody (anti-PD-1 Ab) and the combination (Combination; D35LNP0.5% and anti-PD-1 antibody) showed significant tumor-suppressive effect in both tumor volume (Fig. 5B; left panel) and tumor weight (Fig. 5B; right panel) compared to the isotype antibody control group (Isotype).

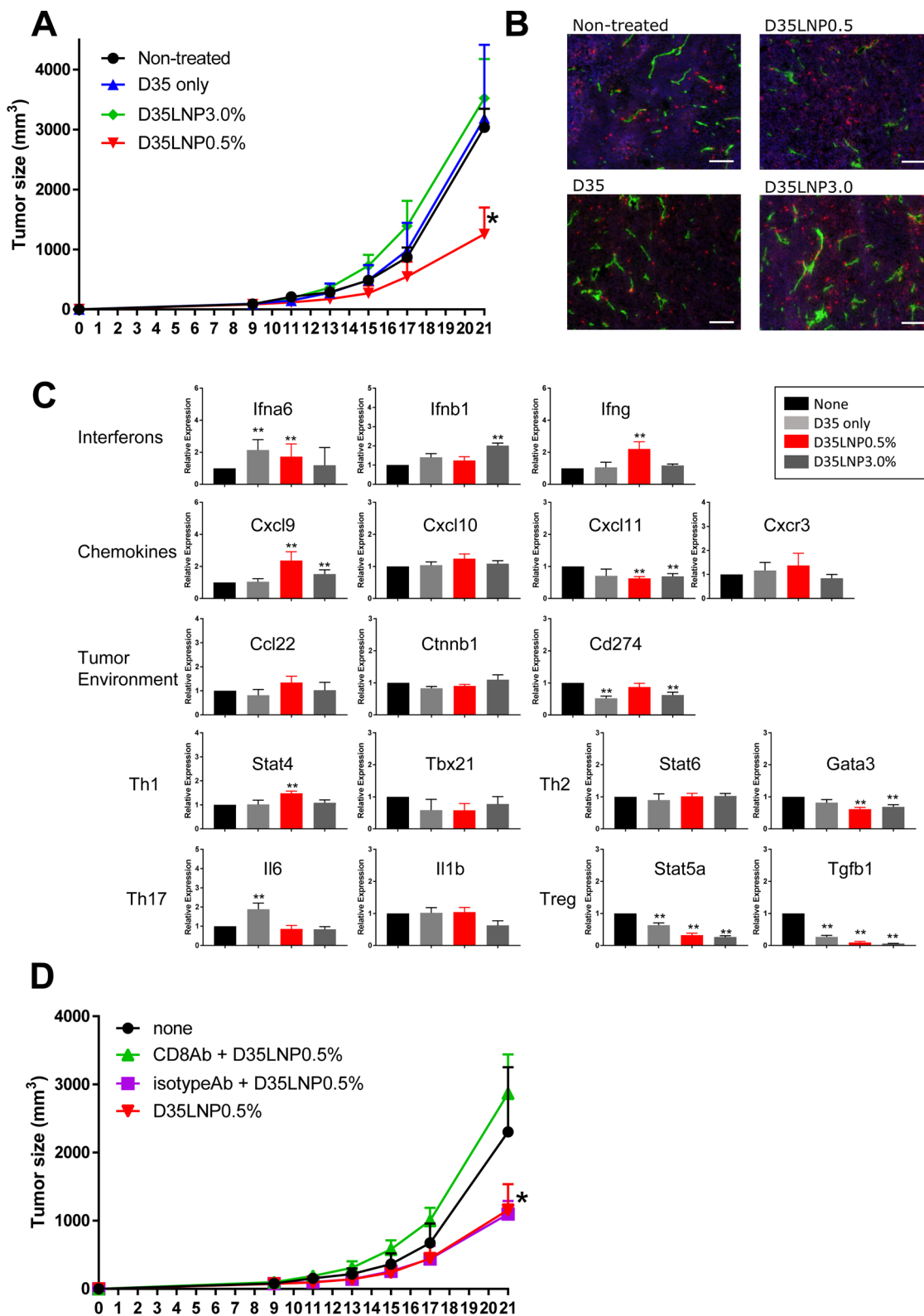


Fig. 4. MC38 tumor growth was also suppressed with D35LNP0.5% intravenous treatment. (A) Tumor growth curve. C57BL/6 mice were injected intradermally with MC38 tumor cells (1×10^6). D35LNP was injected intravenously at days 9, 11, 13, 15 and 17. * $P < 0.05$. Statistical significance was calculated by one-way ANOVA with Bonferroni test. (B) Immuno-fluorescence staining of MC38 tumor for nuclei (DAPI, blue), CD31 (green), and CD8b (red). (C) mRNA expression of the same gene panels as Fig. 3A measured by qRT-PCR method. ** $P < 0.01$. Statistical significance was calculated by Mann-Whitney U test. (D) Tumor growth curve with or without CD8a antibody treatment. * $P < 0.05$. Statistical significance was calculated by one-way ANOVA with Bonferroni test.

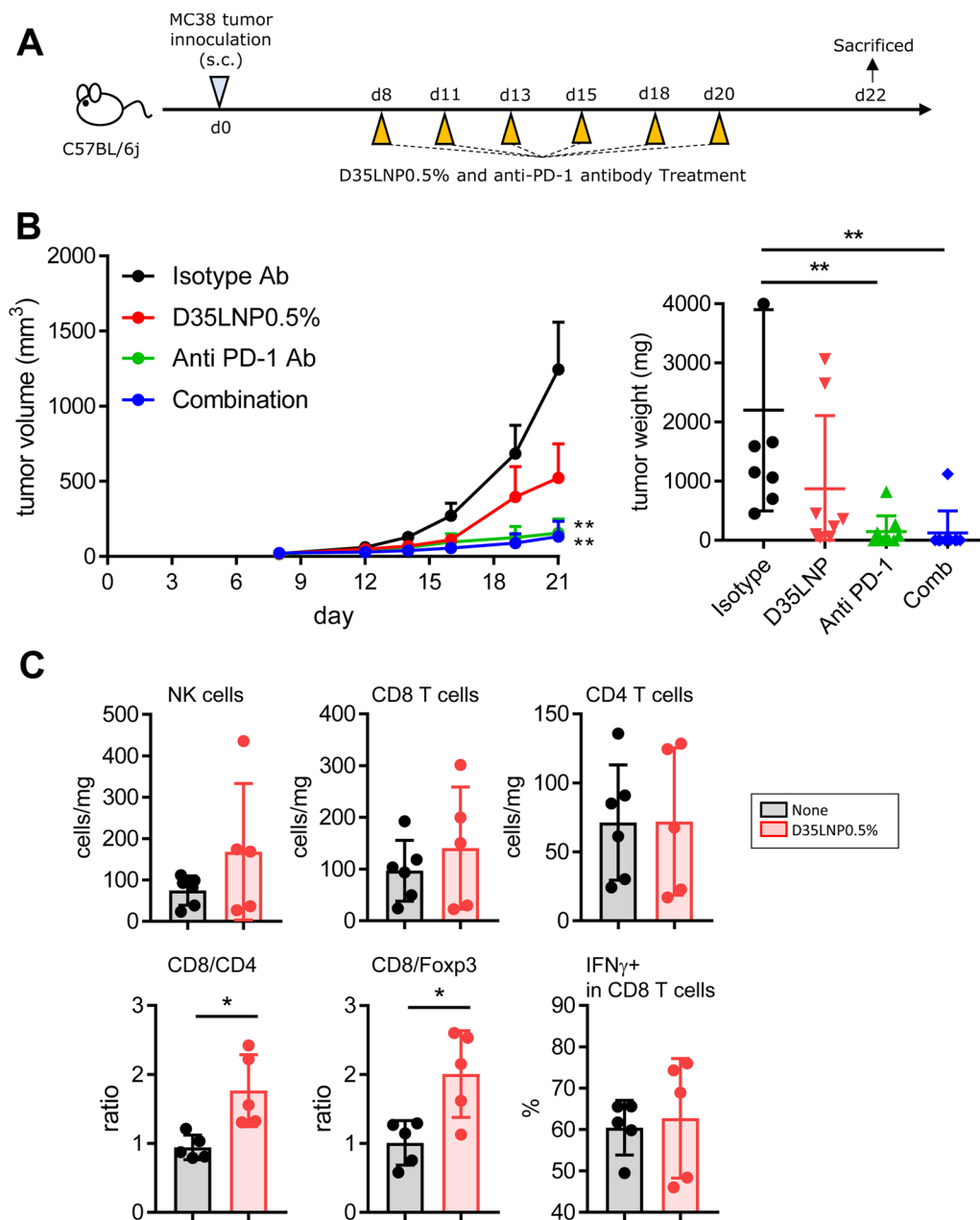


Fig. 5. Intratumoral D35LNP0.5% and anti-PD-1 antibody combination treatment.

(A) Treatment procedure. C57BL/6 mice were injected subcutaneously with MC38 tumor cells (1×10^6). Both D35LNP0.5% and anti-PD-1 antibody were simultaneously injected at days 8, 11, 13, 15, 18, and 20. (B) Tumor volume curves (left) and tumor weight at 22 days after tumor inoculation (right) (Isotype Ab, n = 7; D35LNP0.5%, n = 8; Anti PD-1 Ab, n = 9; Combination, n = 9). Statistical significances were calculated by one-way ANOVA with Tukey multiple comparison test. (C) Immune cell population analysis of tumors by FACS from Isotype Ab (n = 6) vs. D35LNP0.5% treated mice (n = 5). * CD8/4: p = 0.0102, CD8/Foxp3: p = 0.0133. Statistical significances were calculated by Student's t-test

We also investigated immune cell populations in tumors by flow cytometry. The ratio of CD8/CD4 to CD8/Foxp3 in tumor-infiltrating T cells significantly increased in the D35LNP0.5% treated group compared to that in the Isotype group (Fig. 5C). Note that we could not perform immune cell population analysis for the other two groups (anti-PD-1 Ab and Combination), because the tumor samples were too small to recover sufficient numbers of the immune cells.

To further investigate whether this combinational therapeutic effect is affected by the administration route of D35LNP0.5%, we also treated MC38 tumor bearing mice with D35LNP0.5% i.v. and/or PD-1 blocking antibody i.p. using similar protocol as shown in Fig. 5A (3 times a week between 7–19 days after tumor inoculation). The Combination showed significant inhibitory effect on tumor growth compared to that in the Isotype group (Fig. 6A). Although the difference in anti-tumor efficacy between the anti-PD-1 Ab group and the Combination group was not statistically significant (Fig. 6A), the Combination group showed more consistent tumor-suppressive effect in individual mice (Fig. 6B). We also analyzed tumor infiltrating immune cell populations in each group by flow cytometry. The absolute count of CD8 T cells, and both CD8/

CD4 and CD8/Foxp3 ratio significantly increased in the Combination group compared to Isotype and D35LNP groups (Fig. 6C). Regarding the function of CD8 T cells, the Ki-67 positive population significantly increased in the anti-PD-1 Ab group compared to that in the Isotype group (p = 0.0126), and the IFN γ -positive population significantly increased in the Combination group compared to that in the Isotype group (p = 0.0420). (Fig. 6C). While tumor-associated neutrophils (TANs) significantly reduced in the Anti-PD-1 Ab and Combination groups (both contain Anti-PD-1 Ab treatment), inflammatory monocytes (iMonocytes) significantly reduced in the D35LNP0.5% and Combination groups (both contain D35LNP0.5% treatment). These results suggest that the combination of D35LNP0.5% and PD-1 blockade improved anti-tumor effect irrespective of the D35LNP0.5% administration route, and either D35LNP0.5% or PD-1 blockade might have preferentially inhibited different inhibitory myeloid cell populations such as iMonocytes or TANs, respectively (Fig. 6C).

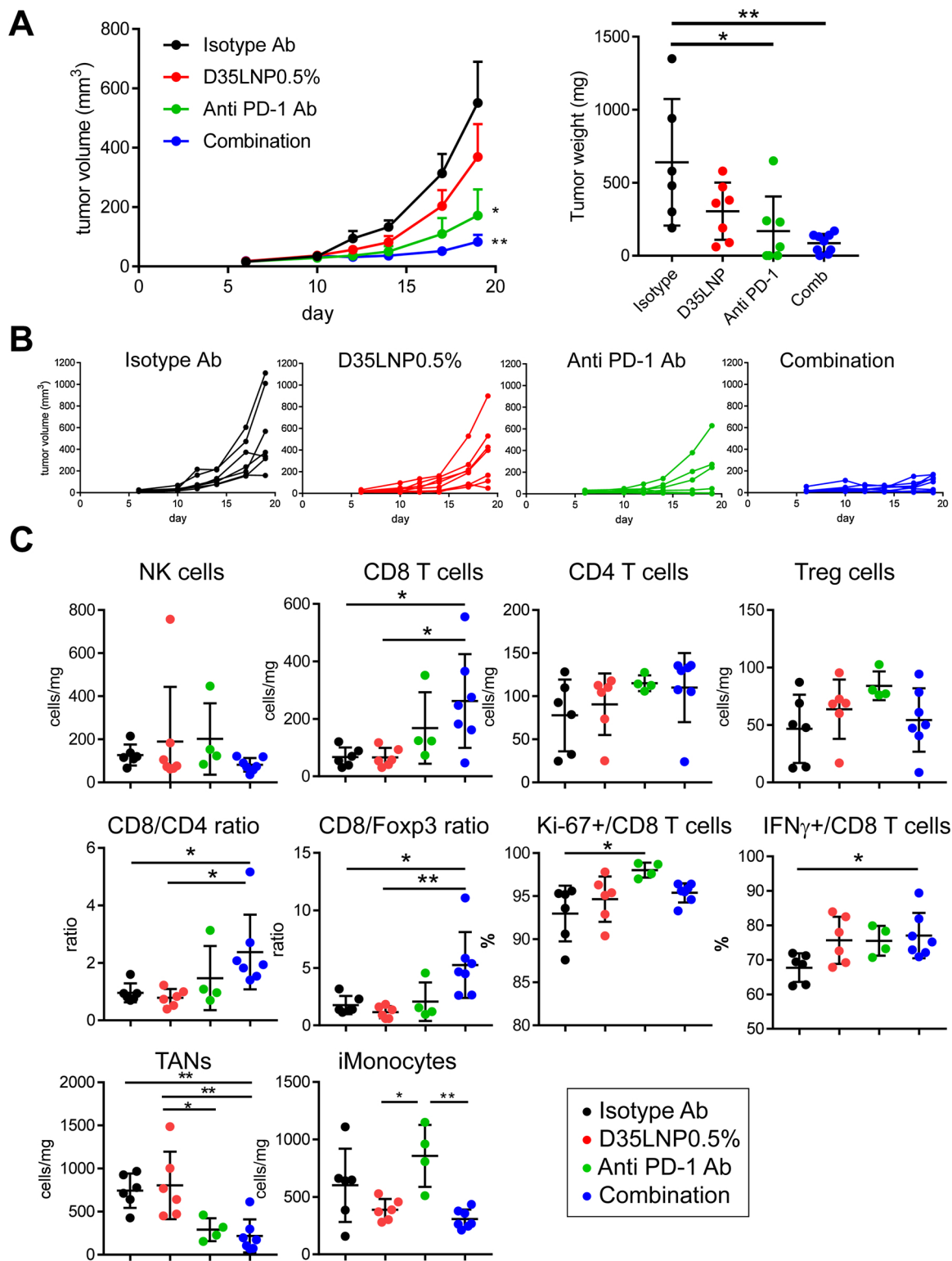


Fig. 6. Intravenous D35LNP0.5% and anti PD-1 antibody combination treatment. (A) Tumor volume curves (left) and tumor weight 20 days after tumor cell inoculation (right) (Isotype Ab, n = 6; D35LNP0.5%, n = 7; Anti PD-1 Ab, n = 7; Combination, n = 9). (Left: * Isotype vs. anti PD-1 p < 0.05; ** Isotype vs. Comb p < 0.01; Right: * Isotype vs. PD-1 only p = 0.0111, ** Isotype vs. Comb p = 0.0014). (B) Tumor volume curves from each mouse in 4 different groups. (C) Immune cell populations were evaluated in each treatment group (*p < 0.05 **p < 0.01). Isotype vs. Comb (CD8 T: p = 0.0192, CD8 T/CD4 T ratio: p = 0.0431, CD8/Foxp3 ratio: p = 0.0129). D35LNP vs Comb (CD8 T: p = 0.0181, CD8 T/CD4 T ratio: p = 0.0207, CD8/Foxp3 ratio: p = 0.0033). All statistical significances were calculated by one-way ANOVA with Tukey multiple comparison test.

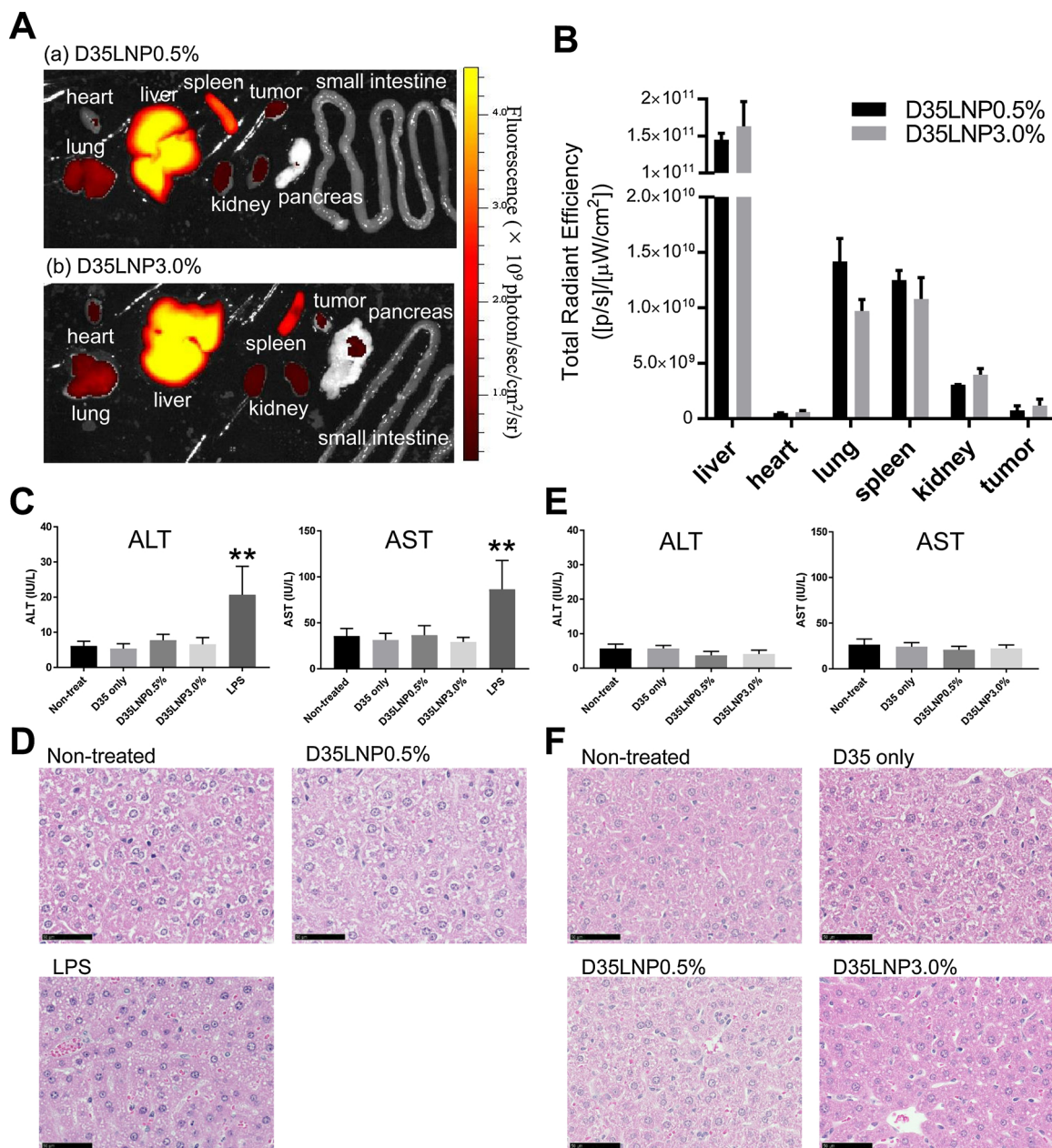


Fig. 7. Tissue distribution and liver toxicity after intravenous D35LNP administration.

(A) DiR fluorescence dye labeled D35LNP0.5% and D35LNP3.0% were administered intravenously. In 6 h later, biodistribution was evaluated by IVIS for the indicated organs. (B) Quantified DiR signals in the indicated organs. (C) ALT and AST in the plasma were evaluated after single D35LNP intravenous administration. $**p < 0.01$. Statistical significance was calculated by one-way ANOVA with Bonferroni test. (D) The liver histology after single D35LNP intravenous administration. Scale bars; 50 μm. (E) ALT and AST in the plasma after 5 times repeated D35LNP intravenous administrations. (F) The liver histology after 5 times repeated D35LNP intravenous administrations. Scale bars; 50 μm.

3.6. Biodistribution and liver toxicity evaluation after D35LNP intravenous administration

To assess the biodistribution, D35LNP, D35LNP0.5% and D35LNP3.0% were labeled with DiR, a near infrared fluorescence dye. At 6 h after intravenous injection, most DiR-labeled D35LNP0.5% and D35LNP3.0% were observed in the reticuloendothelial system and organs such as the liver, the lung, and the spleen (Fig. 7A and B). We also observed DiR signal in tumor tissues, but it was weaker and lesser in intensity than that of the kidney (Fig. 7B). These results suggested that the overall organ distribution of D35LNP0.5% and D35LNP3.0% was almost the same, and ~1.0% of D35LNP reached the tumor after i.v. injection.

Because the liver was the organ with highest D35LNP distribution, we next examined liver toxicity after single or repeated (5 times every 2 days similar to the tumor treatment schedule) i.v. injection of D35LNP0.5% and D35LNP3.0%. After single injection, no elevation in AST and ALT was observed in the plasma compared to LPS, as the liver damage-inducing positive control (Fig. 7C). Consistent with this result, histological examination also showed no apparent liver damage with D35LNP0.5% while the LPS group showed decreased glycogen deposition as shown by the white space reduction in hepatocytes and the appearance of increased small round vacuoles in the cytosol (Fig. 7D). Moreover, no liver damage was observed after repeated D35LNP i.v. injection 5 times within 2 weeks (Fig. 7E and F). These results indicated that the therapeutic schedule and dose of D35LNP i.v. injection did not

induce apparent liver damage in mice.

4. Discussion

Among the 4 different types of CpG ODNs (including A, B, C and P), Type-A CpG is one of the strongest IFN- α inducer, which has been considered a good cytokine for cancer therapy [45,46], and one of the weakest inflammatory IL-6 inducer which potentially promotes tumor progression [47,48]. However, the use of Type-A CpG ODNs for cancer treatment has been limited, because it is prone to degradation and uncontrolled aggregation formation in vivo. To overcome this limitation, we developed D35LNP. D35LNP induced high amount of IFN- α secretion from human PBMC and mouse bone marrow cells (Fig. 1). This IFN- α production was dependent on the presence of CpG motif in D35 ODN sequence, and TLR9 mediated signaling in pDCs (Fig. 1C, E, F, G). Optimal in vitro IFN- α production was achieved by 0.5% of 2k-PEG-lipid incorporation, but 3% of 2k-PEG-lipid incorporation resulted in very weak IFN- α production, suggesting that surface PEG modification greatly influenced D35LNP's activity (Fig. 1A and B).

According to these in vitro results, D35LNP0.5% but not D35LNP3.0% showed anti-tumor effect in vivo. In the MC38 subcutaneous tumor model, tumor growth suppression was dependent on CD8 T cells, irrespective of the administration route of D35LNP0.5% such as i.t. or i.v., suggesting that CD8⁺ T cells work as a final anti-tumor effector cells. T cell repertoire examination also supported that D35LNP treatment induced tumor-specific T cells, which has a significantly skewed TCR repertoire gene expression (such as *Va6-5/6-7* and *Va12*) in the tumor, but not in the spleen (Fig. 3B). The other immune-related tumor mRNA also changed with D35LNP0.5% treatments. As expected, IFN- α response was induced by D35LNP0.5% treatments. mRNA expression levels of interferons (*Iffa6*, *Iffb1*, *Iffng*), CD8 T cell recruitment chemokines and chemokine receptors (*Cxcl9*, *Cxcl10*, *Cxcl11*, and *Cxcr3*), and Th1 related genes (*Stat4* and *Tbx21*) were significantly increased, and their strong induction was associated with tumor suppression after i.t. treatment (Fig. 3A). Similar results were also seen after i.v. treatment (Fig. 4C). Although the expression of these marker genes was higher with i.t. treatment, significant induction of *Iffng* and *Cxcl9* expression after i.v. treatment was associated with tumor-suppressive D35LNP0.5% i.v. treatment but not with tumor non-suppressive D35LNP3.0% i.v. treatment (Fig. 4C). These results suggested that D35LNP treatment changed the tumor microenvironment toward a Th1 and CD8 T cell-activated environment, irrespective of i.t. or i.v. treatment. This Th1/CD8 T cell skewed tumor microenvironment induced by D35LNP administration also enhanced anti-PD-1 antibody's therapeutic effect. D35LNP0.5% and anti-PD-1 antibody combination treatment increased the number of CD8 T cell and IFN- γ ⁺ CD8 T cells, and the ratios of CD8/CD4 and CD8/Foxp3, and elicited more consistent tumor growth suppression (Fig. 6). This suggests that D35LNP0.5% accelerated anti-tumor immunity by inducing Th1/CD8 skewed tumor microenvironment, while anti-PD-1 antibody released the brake on these T cells.

The exact mechanisms of the anti-tumor activity difference between D35LNP0.5% and D35LNP3.0% need further examination. It has been known that PEGylated lipid particles showed two different types of phenomena; "PEG dilemma" [39] and "accelerated blood clearance (ABC) phenomenon" [49]. Theoretically, it is possible that both phenomena influence the difference between D35LNP0.5% and D35LNP3.0%. "PEG dilemma" suggested that PEGylation amount dependent inhibition of cellular uptake, and ABC phenomenon suggested anti-PEG antibody induction dependent rapid clearance of PEGylated lipid particles. Both would result in the biological activity reduction of PEGylated lipid particles in vivo via intravenous administration route. However, when D35LNP was directly injected into tumor, and D35LNP0.5% was more effective than D35LNP3.0% (Fig. 2B). In this case, we may exclude the possibility of ABC phenomenon involvement in the anti-tumor effect reduction of D35LNP3.0%, and PEG dilemma

would be the main reason for the difference of the anti-tumor activity between D35LNP0.5% and D35LNP3.0%.

Although our results clearly showed that D35LNP injection activated anti-tumor immunity in the host, the detailed cellular mechanism in vivo is still not fully elucidated. The key role of pDC in IFN- α induction by D35LNP stimulation in vitro (Fig. 1F and G) strongly suggested that pDC activation by D35LNP should be important in vivo. It has been reported that CpG-activated pDC administration in tumor induced antitumor effect through pDC-NK-cDC-CD8T cell activation where pDC produced CCL3/4/5 and NK cell expressed CCR5 [50]. Another report showed that activated NK cells produced CCL5 and XCL1, and both chemokines were involved in cDC1 recruitment [51]. In another report, activated CD8 T cells have been shown to secrete XCL1 and CCL3/4 to recruit XCR1⁺ cDC1 and CCR5⁺ pDCs, respectively, and to make clusters of CD8 T/pDC/cDC1 for efficient CD8 T cell priming [52]. Tumor residing cDC1 cells also produced CXCL9/CXCL10 to recruit CXCR3⁺ cells [53]. Summarily, these reports suggested that D35LNP-mediated pDC activation provoked these redundant chemokine networks to form NK/pDC/cDC1 clusters for initiating efficient anti-tumor cell responses.

Our created D35LNP showed anti-tumor effect both in i.t. and in i.v. administration routes. This is different from other reported CpG based immune stimulators for cancer immunotherapy, in which only i.t. or s.c. was evaluated [25,54–57]. Although a very small amount of i.v.-administered D35LNP reached the tumor site (Fig. 7A and B), tumor growth suppression with D35LNP i.v. treatment was dependent on CD8 T cells, which was the same with i.t. administration. Based on these facts, we speculated that i.t. and i.v. treatment of D35LNP shared partially similar mechanism of actions. However, expression of Treg-related genes such as *Stat5* and *Tgfb1* increased after i.t. administration (Fig. 3G), but decreased after i.v. administration (Fig. 4C), suggesting that i.v. administration of D35LNP may invoke additional or different systemic actions, and this possibility requires examination in future experiments.

After i.v. treatment, majority of D35LNP accumulated in the reticuloendothelial system (liver, lung, and spleen), which has been known to capture other particulate drugs such as liposomes. Even with high accumulation in the liver, we could not detect any abnormal ALT and AST elevation after D35LNP i.v. administration (Fig. 7C and E). Although the exact reason for this low liver toxicity by D35LNP requires examination in future experiments, natural phosphodiester backbone of D35 may contribute to high safety profile of D35LNP.

Through these developmental processes in this study, we consider that D35LNP0.5% is one of the optimized formulations of D35 for cancer therapy without liver toxicity. Notably, original lipid free D35 did not show any therapeutic effect on cancer in vivo (Fig. 2A and A). Currently, no other CpG-based immunostimulator that can be administered systemically has been reported. Our developed D35LNP formulation suppressed tumor growth after administration through not only i.t. but also with i.v. routes. Combination with anti-PD-1 antibody induced more consistent tumor suppression. Summarily, D35LNP is a promising immunostimulator for future cancer therapy, which can be combined with a variety of other approaches such as chemotherapy and radiation to improve its therapeutic efficacy [58,59].

Author contributions

S.K., R.S., and T.A. designed research, L.M., Y.T., A.O., J.M., and Y.H. conducted the research, Y.N., H.M., A.K., D.O., K.M., Y.Y., and Y.O. contributed critical reagents/tools used for the study, L.M., Y.T., A.O., S.K., R.S., and T.A. analyzed data; and L.M., Y.T., S.K., R.S., and T.A. wrote the paper.

Declaration of Competing Interest

These authors disclose the following: Yasuo Yoshioka and Taiki

Aoshi are employed by the Research Foundation for Microbial Diseases of Osaka University. Shohei Koyama, Ryo Suzuki, and Taiki Aoshi have filed a patent application related to the content of this manuscript. The remaining authors declare no conflicts.

Significance statement

Lipid nanoparticle formulation of Type-A CpG oligodeoxynucleotide D35 enabled the conversion of otherwise in vivo ineffective D35 to tumor suppressive immunomodulatory D35 in vivo. Our formulation could be administered intratumorally or intravenously to induce Th1 and CD8 T cells -skewed immune environment in the host without apparent liver toxicity. Our D35-containing lipid nanoparticles (D35LNP) formulation can be used an immunomodulator for cancer immunotherapy and potentially in the treatment of other diseases that require Th1 and CD8 T cells -skewed immune activation.

Acknowledgments

We thank Yutaka Kono, Toshihiro Nukiwa, and Koichi Yamanishi for useful advices, Miki Tsutsui and Megumi Yamashita for technical assistance, and Saiko Ito for secretary assistance. We acknowledge the financial support from the Japan Agency for Medical Research and Development (AMED) with grant number (16cm0106310h0001, 17cm0106310h0002, 18cm0106310h0003).

Appendix A. Supplementary data

Supplementary material related to this article can be found, in the online version, at doi:<https://doi.org/10.1016/j.jconrel.2019.09.011>.

References

- G. Lizée, W.W. Overwijk, L. Radvanyi, J.J. Gao, P. Sharma, P. Hwu, Harnessing the power of the immune system to target cancer, in: C.T. Caskey (Ed.), *Annual Review of Medicine*, Vol 64 2013, pp. 71–90.
- K.M. Hargadon, C.E. Johnson, C.J. Williams, Immune checkpoint blockade therapy for cancer: an overview of FDA-approved immune checkpoint inhibitors, *Int. Immunopharmacol.* 62 (2018) 29–39.
- J. Gong, A. Chehrzai-Raffle, S. Reddi, R. Sargia, Development of PD-1 and PD-L1 inhibitors as a form of cancer immunotherapy: a comprehensive review of registration trials and future considerations, *J. Immunother. Cancer* 6 (2018).
- T. Floros, A.A. Tarhini, Anticancer cytokines: biology and clinical effects of Interferon-alpha2, interleukin (IL)-2, IL-15, IL-21, and IL-12, *Semin. Oncol.* 42 (2015) 539–548.
- T.A. Waldmann, Cytokines in cancer immunotherapy, *Cold Spring Harb. Perspect. Biol.* 10 (2018).
- M.A. Shetab Boushehri, A. Lamprecht, TLR4-based immunotherapeutics in cancer: a review of the achievements and shortcomings, *Mol. Pharm.* 15 (2018) 4777–4800.
- K.A. Martins, S. Bavari, A.M. Salazar, Vaccine adjuvant uses of poly-IC and derivatives, *Expert Rev. Vaccines* 14 (2015) 447–459.
- C.L. Chiang, L.E. Kandalaf, In vivo cancer vaccination: Which dendritic cells to target and how? *Cancer Treat. Rev.* 71 (2018) 88–101.
- J.S. Weber, J.C. Yang, M.B. Atkins, M.L. Disis, Toxicities of immunotherapy for the practitioner, *J. Clin. Oncol.* 33 (2015) 2092–2099.
- M. Qin, Y. Li, X. Yang, H.Q. Wu, Safety of Toll-like receptor 9 agonists: a systematic review and meta-analysis, *Immunopharmacol. Immunotoxicol.* 36 (2014) 251–260.
- S.E. Krown, D. Kerr, W.E. Stewart 2nd, A.K. Field, H.F. Oettgen, Phase I trials of poly(I,C) complexes in advanced cancer, *J. Biol. Response Mod.* 4 (1985) 640–649.
- D.M. Klinman, Immunotherapeutic uses of CpG oligodeoxynucleotides, *Nat. Rev. Immunol.* 4 (2004) 248–257.
- J. Vollmer, A.M. Krieg, Immunotherapeutic applications of CpG oligodeoxynucleotide TLR9 agonists, *Adv. Drug Deliv. Rev.* 61 (2009) 195–204.
- M. Heikenwalder, M. Polymenidou, T. Junt, C. Sigurdson, H. Wagner, S. Akira, R. Zinkernagel, A. Aguzzi, Lymphoid follicle destruction and immunosuppression after repeated CpG oligodeoxynucleotide administration, *Nat. Med.* 10 (2004) 187–192.
- E.M. Behrens, S.W. Canina, K. Slade, S. Rao, P.A. Kreiger, M. Paessler, T. Kambayashi, G.A. Koretzky, Repeated TLR9 stimulation results in macrophage activation syndrome-like disease in mice, *J. Clin. Invest.* 121 (2011) 2264–2277.
- T. Sparwasser, L. Hultner, E.S. Koch, A. Luz, G.B. Lipford, H. Wagner, Immunostimulatory CpG-oligodeoxynucleotides cause extramedullary murine hemopoiesis, *J. Immunol.* 162 (1999) 2368–2374.
- C. Manegold, N. van Zandwijk, A. Szczesna, P. Zatloukal, J.S. Au, M. Blasinska-Morawiec, P. Serwatowski, M. Krzakowski, J. Jassem, E.H. Tan, R.J. Benner, A. Ingrosso, S.J. Meech, D. Readett, N. Thatcher, A phase III randomized study of gemcitabine and cisplatin with or without PF-3512676 (TLR9 agonist) as first-line treatment of advanced non-small-cell lung cancer, *Ann. Oncol.* 23 (2012) 72–77.
- V. Hirsh, L. Paz-Ares, M. Boyer, R. Rosell, G. Middleton, W.E. Eberhardt, A. Szczesna, P. Reiterer, M. Saleh, O. Arrieta, E. Bajetta, R.T. Webb, J. Raats, R.J. Benner, C. Fowst, S.J. Meech, D. Readett, J.H. Schiller, Randomized phase III trial of paclitaxel/carboplatin with or without PF-3512676 (Toll-like receptor 9 agonist) as first-line treatment for advanced non-small-cell lung cancer, *J. Clin. Oncol.* 29 (2011) 2667–2674.
- D.A. Brown, S.H. Kang, S.M. Gryaznov, L. DeDionisio, O. Heidenreich, S. Sullivan, X. Xu, M.I. Nerenberg, Effect of phosphorothioate modification of oligodeoxynucleotides on specific protein binding, *J. Biol. Chem.* 269 (1994) 26801–26805.
- C.C. Wu, J. Lee, E. Raz, M. Corr, D.A. Carson, Necessity of oligonucleotide aggregation for toll-like receptor 9 activation, *J. Biol. Chem.* 279 (2004) 33071–33078.
- U. Flierl, T.L. Nero, B. Lim, J.F. Arthur, Y. Yao, S.M. Jung, E. Gitz, A.Y. Pollitt, M.T. Zaldivia, M. Jandrot-Perrus, A. Schaefer, B. Nieswandt, R.K. Andrews, M.W. Parker, E.E. Gardiner, K. Peter, Phosphorothioate backbone modifications of nucleotide-based drugs are potent platelet activators, *J. Exp. Med.* 212 (2015) 129–137.
- S.P. Henry, G. Beattie, G. Yeh, A. Chappel, P. Giclas, A. Mortari, M.A. Jagels, D.J. Kornbrust, A.A. Levin, Complement activation is responsible for acute toxicities in rhesus monkeys treated with a phosphorothioate oligodeoxynucleotide, *Int. Immunopharmacol.* 2 (2002) 1657–1666.
- D.R. Shaw, P.K. Rustagi, E.R. Kandimalla, A.N. Manning, Z. Jiang, S. Agrawal, Effects of synthetic oligonucleotides on human complement and coagulation, *Biochem. Pharmacol.* 53 (1997) 1123–1132.
- J.P. Sheehan, H.C. Lan, Phosphorothioate oligonucleotides inhibit the intrinsic tenase complex, *Blood* 92 (1998) 1617–1625.
- F. Bichat, S. Maubant, J.F. Mirjole, P. Slos, A.M. Krieg, A. Morris, Antitumor activity of the CMP-001 (TLR9 agonist) alone or combined with immune modulators in syngeneic tumor models, *Cancer Res.* 77 (2017).
- Y. Lou, C. Liu, G. Lizée, W. Peng, C. Xu, Y. Ye, B.A. Rabinovich, Y. Hailemichael, A. Gelbard, D. Zhou, W.W. Overwijk, P. Hwu, Antitumor activity mediated by CpG: the route of administration is critical, *J. Immunother.* 34 (2011) 279–288.
- D. Verthelyi, K.J. Ishii, M. Gursel, F. Takeshita, D.M. Klinman, Human peripheral blood cells differentially recognize and respond to two distinct CPG motifs, *J. Immunol.* 166 (2001) 2372–2377.
- T. Aoshi, Y. Haseda, K. Kobiyama, H. Narita, H. Sato, H. Nankai, S. Mochizuki, K. Sakurai, Y. Katakai, Y. Yasutomi, E. Kuroda, C. Coban, K.J. Ishii, Development of nonaggregating poly-A tailed immunostimulatory A/D type CpG oligodeoxynucleotides applicable for clinical use, *J. Immunol. Res.* 2015 (2015) 316364.
- M. Kerkmann, L.T. Costa, C. Richter, S. Rothenfusser, J. Battiany, V. Hornung, J. Johnson, S. Englert, T. Ketterer, W. Heckl, S. Thallhammer, S. Endres, G. Hartmann, Spontaneous formation of nucleic acid-based nanoparticles is responsible for high interferon-alpha induction by CpG-A in plasmacytoid dendritic cells, *J. Biol. Chem.* 280 (2005) 8086–8093.
- Q. Zhao, S. Matson, C.J. Herrera, E. Fisher, H. Yu, A.M. Krieg, Comparison of cellular binding and uptake of antisense phosphodiester, phosphorothioate, and mixed phosphorothioate and methylphosphonate oligonucleotides, *Antisense Res. Dev.* 3 (1993) 53–66.
- E. Blanco, H. Shen, M. Ferrari, Principles of nanoparticle design for overcoming biological barriers to drug delivery, *Nat. Biotechnol.* 33 (2015) 941–951.
- S. Chen, L.F. Lee, T.S. Fisher, B. Jessen, M. Elliott, W. Evering, K. Logronio, G.H. Tu, K. Tsaparikos, X. Li, H. Wang, C. Ying, M. Xiong, T. Vanarsdale, J.C. Lin, Combination of 4-1BB agonist and PD-1 antagonist promotes antitumor effector/memory CD8 T cells in a poorly immunogenic tumor model, *Cancer Immunol. Res.* 3 (2015) 149–160.
- S.F. Ngiow, B. von Scheidt, H. Akiba, H. Yagita, M.W.L. Teng, M.J. Smyth, Anti-TIM3 antibody promotes t cell IFN- γ -mediated antitumor immunity and suppresses established tumors, *Cancer Res.* 71 (2011) 3540–3551.
- R. Suzuki, Y. Oda, D. Omata, N. Nishiie, R. Koshima, Y. Shiono, Y. Sawaguchi, J. Unga, T. Naoi, Y. Negishi, S. Kawakami, M. Hashida, K. Maruyama, Tumor growth suppression by the combination of nanobubbles and ultrasound, *Cancer Sci.* 107 (2016) 217–223.
- M.W. Pfaffl, A new mathematical model for relative quantification in real-time RT-PCR, *Nucleic Acids Res.* 29 (2001) e45.
- P. Dash, J.L. McClaren, T.H. Oguin 3rd, W. Rothwell, B. Todd, M.Y. Morris, J. Becksfort, C. Reynolds, S.A. Brown, P.C. Doherty, P.G. Thomas, Paired analysis of TCRalpha and TCRbeta chains at the single-cell level in mice, *J. Clin. Invest.* 121 (2011) 288–295.
- E.A. Akbay, S. Koyama, Y. Liu, R. Dries, L.E. Bufe, M. Silkes, M.M. Alam, D.M. Magee, R. Jones, M. Jinushi, M. Kulkarni, J. Carretero, X. Wang, T. Warner-Hatten, J.D. Cavanaugh, A. Osa, A. Kumanogoh, G.J. Freeman, M.M. Awad, D.C. Christiani, R. Bueno, P.S. Hammerman, G. Dranoff, K.K. Wong, Interleukin-17A promotes lung tumor progression through neutrophil attraction to tumor sites and mediating resistance to PD-1 blockade, *J. Thorac. Oncol.* 12 (2017) 1268–1279.
- S. Koyama, E.A. Akbay, Y.Y. Li, A.R. Aref, F. Skoulidis, G.S. Herter-Sprie, K.A. Buczkowski, Y. Liu, M.M. Awad, W.L. Denning, L. Diao, J. Wang, E.R. Parra-Cuentas, I.I. Wistuba, M. Soucheray, T. Thai, H. Asahina, S. Kitajima, A. Altabel, J.D. Cavanaugh, K. Rhee, P. Gao, H. Zhang, P.E. Fecci, T. Shimamura, M.D. Hellmann, J.V. Heymach, F.S. Hodi, G.J. Freeman, D.A. Barbie, G. Dranoff, P.S. Hammerman, K.K. Wong, STK11/LKB1 deficiency promotes neutrophil recruitment and proinflammatory cytokine production to suppress T-cell activity in the lung tumor microenvironment, *Cancer Res.* 76 (2016) 999–1008.
- H. Hatakeyama, H. Akita, H. Harashima, The polyethyleneglycol dilemma:

- advantage and disadvantage of PEGylation of liposomes for systemic genes and nucleic acids delivery to tumors, *Biol. Pharm. Bull.* 36 (2013) 892–899.
- [40] X.W. Cheng, R.J. Lee, The role of helper lipids in lipid nanoparticles (LNPs) designed for oligonucleotide delivery, *Adv. Drug Deliv. Rev.* 99 (2016) 129–137.
- [41] M. Ayers, J. Luceford, M. Nebozhyn, E. Murphy, A. Loboda, D.R. Kaufman, A. Albright, J.D. Cheng, S.P. Kang, V. Shankaran, S.A. Piha-Paul, J. Yearley, T.Y. Seiwert, A. Ribas, T.K. McClanahan, IFN-gamma-related mRNA profile predicts clinical response to PD-1 blockade, *J. Clin. Invest.* 127 (2017) 2930–2940.
- [42] R. Cristescu, R. Mogg, M. Ayers, A. Albright, E. Murphy, J. Yearley, X. Sher, X.Q. Liu, H. Lu, M. Nebozhyn, C. Zhang, J.K. Luceford, A. Joe, J. Cheng, A.L. Webber, N. Ibrahim, E.R. Plimack, P.A. Ott, T.Y. Seiwert, A. Ribas, T.K. McClanahan, J.E. Tomassini, A. Loboda, D. Kaufman, Pan-tumor genomic biomarkers for PD-1 checkpoint blockade-based immunotherapy, *Science* 362 (2018).
- [43] S. Spranger, Mechanisms of tumor escape in the context of the T-cell-inflamed and the non-T-cell-inflamed tumor microenvironment, *Int. Immunol.* 28 (2016) 383–391.
- [44] S. Spranger, R.M. Spaepen, Y. Zha, J. Williams, Y. Meng, T.T. Ha, T.F. Gajewski, Up-regulation of PD-L1, IDO, and T(regs) in the melanoma tumor microenvironment is driven by CD8(+) T cells, *Sci. Transl. Med.* 5 (2013) 200ra116.
- [45] R.F.V. Medrano, A. Hunger, S.A. Mendonca, J.A.M. Barbuto, B.E. Strauss, Immunomodulatory and antitumor effects of type I interferons and their application in cancer therapy, *Oncotarget* 8 (2017) 71249–71284.
- [46] B.S. Parker, J. Rautela, P.J. Hertzog, Antitumor actions of interferons: implications for cancer therapy, *Nat. Rev. Cancer* 16 (2016) 131–144.
- [47] K. Taniguchi, M. Karin, IL-6 and related cytokines as the critical lynchpins between inflammation and cancer, *Semin. Immunol.* 26 (2014) 54–74.
- [48] D.E. Johnson, R.A. O’Keefe, J.R. Grandis, Targeting the IL-6/JAK/STAT3 signalling axis in cancer, *Nat. Rev. Clin. Oncol.* 15 (2018) 234–248.
- [49] M. Mohamed, A.S. Abu Lila, T. Shimizu, E. Alaaeldin, A. Hussein, H.A. Sarhan, J. Szebeni, T. Ishida, PEGylated liposomes: immunological responses, *Sci. Technol. Adv. Mater.* 20 (2019) 710–724.
- [50] C. Liu, Y. Lou, G. Lizee, H. Qin, S. Liu, B. Rabinovich, G.J. Kim, Y.H. Wang, Y. Ye, A.G. Sikora, W.W. Overwijk, Y.J. Liu, G. Wang, P. Hwu, Plasmacytoid dendritic cells induce NK cell-dependent, tumor antigen-specific T cell cross-priming and tumor regression in mice, *J. Clin. Invest.* 118 (2008) 1165–1175.
- [51] J.P. Bottcher, E. Bonavita, P. Chakravarty, H. Blees, M. Cabeza-Cabrerizo, S. Sammiceli, N.C. Rogers, E. Sahai, S. Zelenay, C. Reis e Sousa, NK cells stimulate recruitment of cDC1 into the tumor microenvironment promoting cancer immune control, *Cell* 172 (2018) 1022–1037 e1014.
- [52] A. Brewitz, S. Eickhoff, S. Dahling, T. Quast, S. Bedoui, R.A. Kroczeck, C. Kurts, N. Garbi, W. Barchet, M. Iannacone, F. Klauschen, W. Kolanus, T. Kaisho, M. Colonna, R.N. Germain, W. Kastanmuller, CD8(+) T cells orchestrate pDC-XCR1(+) dendritic cell spatial and functional cooperativity to optimize priming, *Immunity* 46 (2017) 205–219.
- [53] S. Spranger, D. Dai, B. Horton, T.F. Gajewski, Tumor-residing Batf3 dendritic cells are required for effector T cell trafficking and adoptive t cell therapy, *Cancer Cell* 31 (2017) 711–723 e714.
- [54] D. Wang, W. Jiang, F. Zhu, X. Mao, S. Agrawal, Modulation of the tumor micro-environment by intratumoral administration of IMO-2125, a novel TLR9 agonist, for cancer immunotherapy, *Int. J. Oncol.* 53 (2018) 1193–1203.
- [55] M. Thomas, S. Ponce-Aix, A. Navarro, J. Riera-Knorrenschild, M. Schmidt, E. Wiegert, K. Kapp, B. Wittig, C. Mauri, M.D. Gomez, J. Kollmeier, P. Sadjadian, K.P. Frohling, R.M. Huber, M. Wolf, G. Pall, V. Surmont, L. Bosquee, P. Germonpre, W. Bruckl, C. Grah, C. Herzmann, R. Leistner, A. Meyer, L. Muller, O. Schmalz, C. Scholz, M. Schroder, M. Serke, C. Wesseler, C. Brandts, H.G. Kopp, W. Blau, F. Griesinger, M.R.G. Campelo, Y.G. Garcia, J.M.T. Perez, I.S. Team, Immunotherapeutic maintenance treatment with toll-like receptor 9 agonist leflotolimod in patients with extensive-stage small-cell lung cancer: results from the exploratory, controlled, randomized, international phase II IMPULSE study, *Ann. Oncol.* 29 (2018) 2076–2084.
- [56] S. Wang, J. Campos, M. Gallotta, M. Gong, C. Crain, E. Naik, R.L. Coffman, C. Guiducci, Intratumoral injection of a CpG oligonucleotide reverts resistance to PD-1 blockade by expanding multifunctional CD8+ T cells, *Proc. Natl. Acad. Sci. U. S. A.* 113 (2016) E7240–E7249.
- [57] I. Sagiv-Barfi, D.K. Czerwinski, S. Levy, I.S. Alam, A.T. Mayer, S.S. Gambhir, R. Levy, Eradication of spontaneous malignancy by local immunotherapy, *Sci. Transl. Med.* 10 (2018).
- [58] T.B. Dar, R.M. Henson, S.L. Shiao, Targeting innate immunity to enhance the efficacy of radiation therapy, *Front. Immunol.* 9 (2019).
- [59] B. Jahrsdorfer, G.J. Weiner, CpG oligodeoxynucleotides as immunotherapy in cancer, *Update Cancer Ther.* 3 (2008) 27–32.